Finite-difference-based multiple-relaxation-times lattice Boltzmann model for binary mixtures

Lin Zheng, Zhaoli Guo,* Baochang Shi, and Chuguang Zheng
National Laboratory of Coal Combustion, Huazhong University of Science and Technology, Wuhan 430074, People's Republic of China
(Received 8 June 2009; revised manuscript received 6 October 2009; published 20 January 2010)

In this paper, we propose a finite-difference-based lattice Boltzmann equation (LBE) model with multiple-relaxation times (MRT), in which the distribution functions of individual species evolve on a same regular lattice without any interpolations. Furthermore, the use of the MRT enables the model more flexible so that it can be applied to mixtures of species with different viscosities and adjustable Schmidt number. Some numerical tests are conducted to validate the model, the numerical results are found to agree well with analytical solutions/or other numerical results, and good numerical stability of the proposed LBE model is also observed.

DOI: 10.1103/PhysRevE.81.016706 PACS number(s): 47.11.−j, 44.05.+e

I. INTRODUCTION

Diffusion process plays an important role in many practical applications such as enhanced oil recovery, chemical reactions, pollutant dispersion. Owing to the presence of complex geometries and/or multiple phases with large range of time and space scales appearing in these systems, it is difficult for the traditional methods based on the Navier-Stokes equations to describe the diffusion phenomena. On the other hand, it is well understood that diffusion on the macroscopic level is the result of microscopic interactions between molecules. Therefore, if we can design a model to describe these microscopic interactions correctly at the microscopic level, the macroscopic diffusion phenomena can be captured. The lattice Boltzmann equation (LBE) method is one of such mesoscopic models, and has shown great potentials for simulating such complex systems [1–3].

In the literature, LBE has been successfully applied to single component flows, while for binary mixtures it still needs more clarifications. Although some LBE models [4–21] have been proposed for binary mixtures, most of them [4–13] are based on single-fluid approach with a Bhatnagar-Gross-Krook (BGK) collision operator [22,23]. In this approach, the averaged effect due to the collisions between molecules is described by a total effective BGK collision operator and each species is forced to relax toward the mixture equilibrium state. However, the use of BGK approximation usually leads to fixed Prandtl and Schmidt numbers. To overcome these limitations, some LBE models [14–21] based on two-fluid approach have been proposed, in which each species relaxes to its equilibrium, and some cross couplings between different species are included in the evolution of each species. For instances, some force coupling LBE models [14,15] have been proposed based on a linearized kinetic theory [24]. Alternatively, in Refs. [18,19], the authors proposed a binary and a multicomponent LBE models based on the concept of quasiequilibrium, respectively. Both models have an adjustable Schmidt number, but when the local Schmidt number is higher or lower than a critical value, the quasiequilibrium for each species must be changed locally.

Recently, Asinari [20] pointed out that it was important to consider the indifferentiability principle [25] in LBE for binary mixtures. With this in mind, he proposed a viscous coupling two-fluid LBE model based on Hamel's model [26], and further developed a LBE model with multiple-relaxation times (MRT) [21]. In both models, two collision operators are used to describe the self-collision and cross-collision between particles, respectively. However, as pointed out in Ref. [13], for mixtures consisting of more than two species, it would be rather tedious to describe the cross-collision terms among different species at the same time. Therefore, they regrouped the split-collisional terms into one global collision operator which was virtually a redefinition of the local species equilibrium. Nevertheless, this MRT model is limited to mixtures with identical individual viscosities.

Another problem in most of the existing LBE models for binary mixtures comes from the difference of molecular weights. As known, in LBE the particle speeds of different species depend on the molecular weights. Therefore, the formulation of standard LBE for single-component fluids should be modified to reflect this difference. In the literature three strategies have been proposed to this end, i.e., modified-equilibrium method [5,13,21], two-lattices method [16,18], and finite-difference (FD) method [8,15]. In modified-equilibrium models the standard equilibrium distribution function is reformulated by making the ratio of rest to moving particles adjustable according to the molecular weights. With such a modification, the particles of different species can move on the same lattice. However, this type of LBE models usually leads to identical individual shear viscosities [13,21]. In the two-lattice models [16,18], particles of different species evolve on two lattices with different grid spacing, and interpolation is necessary during the evolution. The FD-LBE models utilize some FD schemes to describe the evolutions of both species so that one same lattice can be used. In the model of Ref. [8], the particle collisions are conducted as usual, but a Lax-Wendroff scheme is employed to implement the streaming process. However, the shear viscosity and diffusivity of the model cannot be tuned freely due to the use of single-fluid formulation with the BGK model. On the other hand, the model in Ref. [15] solves the discrete velocity model based on a two-fluid formulation for mixtures using an upwind scheme.

In this paper, we aim to propose an alternative LBE model for binary mixtures with different molecular weights. The

*Corresponding author; zlguo@hust.edu.cn

model adopts a global MRT collision operator and realizes the streaming process with the Lax-Wendroff scheme. The MRT collision enables the model to be applicable to mixtures with different individual viscosities and an adjustable Schmidt number, while the use of the Lax-Wendroff scheme makes the particles to be able to stream on the same lattice.

The rest of the paper is organized as follows. In Sec. II, the model is described, and a detailed Chapman-Enskog procedure analysis is proposed in Sec. III; boundary conditions for the model are discussed in Sec. IV; some numerical tests are conducted in Sec. V, and finally a brief summary is presented in Sec.VI.

II. MULTIPLE-RELAXATION-TIME LATTICE BOLTZMANN MODEL

Without loss of generality, here we consider two-dimensional flows. A discrete velocity Boltzmann equation with MRT collision operator for a binary mixture fluid can be written as

$$\frac{\partial f_{\sigma i}}{\partial t} + \boldsymbol{c}_{\sigma i} \cdot \nabla f_{\sigma i} = \sum_{\varsigma=a,b} \boldsymbol{S}_{\sigma\varsigma}(f_{\sigma i} - f_{\sigma\varsigma i}^{(eq)}) + F_{\sigma i}, \quad (\sigma = a,b), \tag{1}$$

where $f_{\sigma i}(\boldsymbol{x},t)$ is the distribution function for species σ moving with a discrete velocity $\boldsymbol{c}_{\sigma i}$ at point $\boldsymbol{x}$ and time t, $\boldsymbol{S}_{\sigma\sigma}$ is the self-collision matrix, $\boldsymbol{S}_{\sigma\sigma'}$ is the cross-collision matrix between species σ and σ' $(\sigma \neq \sigma')$, $F_{\sigma i}$ is the forcing term accounting for external body force, $f_{\sigma\varsigma i}^{(eq)}$ is the equilibrium distribution function given by

$$f_{\sigma\varsigma i}^{(eq)} = \frac{\rho_\sigma}{2\pi R_\sigma T_{\sigma\varsigma}^{(eq)}} \exp\left[- \frac{(\boldsymbol{c}_{\sigma i} - \boldsymbol{u}_{\sigma\varsigma}^{(eq)})^2}{2R_\sigma T_{\sigma\varsigma}^{(eq)}} \right],$$

where ρ_σ is the density of species σ, $R_\sigma = k_B/m_\sigma$ (k_B is the Boltzmann constant, m_σ is the mass weight), $\boldsymbol{u}_{\sigma\varsigma}^{(eq)}$ and $T_{\sigma\varsigma}^{(eq)}$ are the parameters that are not necessarily the fluid velocity and temperature, respectively. Considering the irreversible thermodynamics and the Onsager relation [27], one can take $\boldsymbol{u}_{\sigma\sigma'}^{(eq)} = \boldsymbol{u}$ and $T_{\sigma\sigma'}^{(eq)} = T$, where $\boldsymbol{u}$ and T are the velocity and temperature of the mixture. It should be mentioned that the definitions of $\boldsymbol{u}$ and T are the key issues in BGK models. In order to be consistent with the results of the full Boltzmann equations, the following definitions should be used [28]:

$$\boldsymbol{u} = \boldsymbol{u}_{\sigma\sigma'}^{(eq)} = \frac{m_\sigma \boldsymbol{u}_\sigma + m_{\sigma'} \boldsymbol{u}_{\sigma'}}{m_\sigma + m_{\sigma'}}, \tag{2a}$$

$$T = T_{\sigma\sigma'}^{(eq)} = T_\sigma + \frac{2m_\sigma m_{\sigma'}}{(m_\sigma + m_{\sigma'})^2} \left[(T_{\sigma'} - T_\sigma) + \frac{m_{\sigma'}}{6k_B} (\boldsymbol{u}_{\sigma'} - \boldsymbol{u}_\sigma)^2 \right], \tag{2b}$$

where $\boldsymbol{u}_\sigma$ and T_σ are the velocity and temperature of the species σ. However, as pointed out in Ref. [25], if the mixture is consist of identical species, the above definition of $\boldsymbol{u}$ for the BGK models contradicts the indifferentiability principle, and in Ref. [13] the authors argued that the indifferentiablity principle is more important for the hydrodynamic modeling of the mixtures. With this in mind, to maintain the indifferentiability principle, we use the following definition of the mixture velocity

$$\boldsymbol{u} = \frac{\rho_\sigma \boldsymbol{u}_\sigma + \rho_{\sigma'} \boldsymbol{u}_{\sigma'}}{\rho_\sigma + \rho_{\sigma'}}. \tag{3}$$

For mixtures consisting of more than two species, it would be rather tedious to describe the cross-collision terms among different species in Eq. (1), which was also noticed in Ref. [13]. Therefore, in the present study we will choose $\boldsymbol{u}_{\sigma\varsigma}^{(eq)} = \boldsymbol{u}$, and assume the mixture is isothermal, i.e., $T_{\sigma\varsigma}^{(eq)} = T$, just as adopted in previous studies [8,13,22]. With these assumptions we can combine the self-collision term and cross-collision term into a global one, in which the effect of the cross collision is included through the barycentric velocity $\boldsymbol{u}$ in the equilibrium distribution function [8,13,22]. With the above arguments, the discrete velocity model (DVM) [Eq. (1)] can be written as

$$\frac{\partial f_{\sigma i}}{\partial t} + \boldsymbol{c}_{\sigma i} \cdot \nabla f_{\sigma i} = \boldsymbol{S}_\sigma (f_{\sigma i} - f_{\sigma i}^{(eq)}) + F_{\sigma i}, \tag{4}$$

where $\boldsymbol{S}_\sigma = \Sigma_\varsigma \boldsymbol{S}_{\sigma\varsigma}$ is an effective collision matrix, and the global equilibrium distribution function $f_{\sigma i}^{(eq)}$ and the forcing term $F_{\sigma i}$ are, respectively, given by [29,30]

$$f_{\sigma i}^{(eq)} = \omega_i \rho_\sigma \left\{ 1 + \frac{\boldsymbol{c}_{\sigma i} \cdot \boldsymbol{u}}{R_\sigma T} + \frac{1}{2} \left[\frac{(\boldsymbol{c}_{\sigma i} \cdot \boldsymbol{u})^2}{(R_\sigma T)^2} - \frac{(\boldsymbol{u} \cdot \boldsymbol{u})}{R_\sigma T} \right] \right\},$$

$$F_{\sigma i} = \omega_i \rho_\sigma \left[\frac{\boldsymbol{c}_{\sigma i} \cdot \boldsymbol{a}_\sigma}{R_\sigma T} + \frac{(\boldsymbol{c}_{\sigma i} \cdot \boldsymbol{u})(\boldsymbol{c}_{\sigma i} \cdot \boldsymbol{a}_\sigma)}{(R_\sigma T)^2} - \frac{\boldsymbol{a}_\sigma \cdot \boldsymbol{u}}{R_\sigma T} \right], \tag{5}$$

where ω_i are weights associated with the discrete velocities, and $\boldsymbol{a}_\sigma$ is the corresponding external force acceleration. In this work we will consider the two-dimensional nine-velocity (D2Q9) model, in which the discrete velocities for each species are given by $\boldsymbol{c}_{\sigma i} = c_\sigma \boldsymbol{c}_i$ with $c_\sigma = \sqrt{3R_\sigma T}$ being the molecular speed for species σ and

$$\boldsymbol{c}_i = \begin{cases} (0,0), & i = 0 \\ (\cos[(i-1)\pi/2], \sin[(i-1)\pi/2]), & i = 1-4 \\ (\cos[(2i-9)\pi/4], \sin[(2i-9)\pi/4])\sqrt{2}, & i = 5-8 \end{cases} \tag{6}$$

The corresponding weights of the D2Q9 model are defined as $\omega_0 = 4/9$, $\omega_{1-4} = 1/9$ and $\omega_{5-8} = 1/36$.

The densities of each species and the gas properties of mixtures (ρ and $\boldsymbol{u}$) are defined respectively as the velocity moments of distribution functions

$$\rho_\sigma = \sum_i f_{\sigma i}, \quad \rho = \sum_\sigma \rho_\sigma, \quad \rho \boldsymbol{u} = \sum_{\sigma i} c_{\sigma i} f_{\sigma i}, \tag{7}$$

We now solve the evolution equation [Eq. (4)] using a time-splitting scheme, then Eq. (4) can be decomposed into two subprocesses, i.e., the collision process,

$$\frac{\partial f_{\sigma i}}{\partial t} = S_\sigma (f_\sigma - f_\sigma^{(eq)}) + F_{\sigma i}, \tag{8}$$

and the streaming process,

$$\frac{\partial f_{\sigma i}}{\partial t} + c_{\sigma i} \cdot \nabla f_{\sigma i} = 0, \tag{9}$$

As shown in Refs. [31–34], the collision subprocess can be carried out in the moment space. To this end, we first define some moments $\boldsymbol{m}_\sigma$ based on the distributions $f_\sigma(\boldsymbol{x},t)$ through a linear transformation,

$$\boldsymbol{m}_\sigma = \boldsymbol{M} f_\sigma = [m_{\sigma 0}, m_{\sigma 1}, \cdots, m_{\sigma 8}]^T,$$

$$f_\sigma = \boldsymbol{M}^{-1} \boldsymbol{m}_\sigma = [f_{\sigma 0}, f_{\sigma 1}, \cdots, f_{\sigma 8}]^T,$$

where $\boldsymbol{M}$ is a linear transformation given as [32],

$$\boldsymbol{M} = \begin{pmatrix} 1 & 1 & 1 & 1 & 1 & 1 & 1 & 1 & 1 \\ -4 & -1 & -1 & -1 & -1 & 2 & 2 & 2 & 2 \\ 4 & -2 & -2 & -2 & -2 & 1 & 1 & 1 & 1 \\ 0 & 1 & 0 & -1 & 0 & 1 & -1 & -1 & 1 \\ 0 & -2 & 0 & 2 & 0 & 1 & -1 & -1 & 1 \\ 0 & 0 & 1 & 0 & -1 & 1 & 1 & -1 & -1 \\ 0 & 0 & -2 & 0 & 2 & 1 & 1 & -1 & -1 \\ 0 & 1 & -1 & 1 & -1 & 0 & 0 & 0 & 0 \\ 0 & 0 & 0 & 0 & 0 & 1 & -1 & 1 & -1 \end{pmatrix}. \tag{10}$$

With the above relations, the collision process [Eq. (8)] can be mapped onto moment space as

$$\frac{\partial \boldsymbol{m}_\sigma}{\partial t} = \tilde{\boldsymbol{S}}_\sigma (\boldsymbol{m}_\sigma - \boldsymbol{m}_\sigma^{(eq)}) + \tilde{F}_\sigma. \tag{11}$$

Discretizating the above equation using the explicit first order Euler scheme leads to

$$\boldsymbol{m}_\sigma^+ = \boldsymbol{m}_\sigma - \delta t \tilde{\boldsymbol{S}}_\sigma (\boldsymbol{m}_\sigma - \boldsymbol{m}_\sigma^{(eq)}) + \delta t \tilde{F}_\sigma, \tag{12}$$

where $\boldsymbol{m}_\sigma^+ = \boldsymbol{M} f_\sigma^+$ is the postcollision moments with f_σ^+ being the postcollision distribution function, $\tilde{F}_\sigma = \boldsymbol{M} F_\sigma$ is the moments of the forcing term, $\tilde{\boldsymbol{S}}_\sigma = \boldsymbol{M} \boldsymbol{S}_\sigma \boldsymbol{M}^{-1}$ is the corresponding relaxation matrix,

$$\tilde{\boldsymbol{S}}_\sigma = diag\{\tilde{s}_{\sigma 1}, \tilde{s}_{\sigma 2}, \cdots, \tilde{s}_{\sigma 9}\}, \tag{13}$$

where $\tilde{s}_{\sigma i}$ $(i=1-9)$ is the relaxation rate for species σ, and $\boldsymbol{m}_\sigma^{(eq)} = \boldsymbol{M} f_\sigma^{(eq)}$ is the equilibrium in the moment space,

$$\boldsymbol{m}_\sigma^{(eq)} = \boldsymbol{M} f_\sigma^{(eq)} = \begin{pmatrix} \rho_\sigma \\ \rho_\sigma(-2 + 3u^2/c_\sigma^2) \\ \rho_\sigma(1 - 3u^2/c_\sigma^2) \\ \rho_\sigma u_x / c_\sigma \\ -\rho_\sigma u_x / c_\sigma \\ \rho_\sigma u_y / c_\sigma \\ -\rho_\sigma u_y / c_\sigma \\ \rho_\sigma (u_x^2 - u_y^2)/c_\sigma^2 \\ \rho_\sigma (u_x u_y)/c_\sigma^2 \end{pmatrix}. \tag{14}$$

For the streaming process, several methods [8,16,18] have been proposed to solve this convection equation. For instance, in Refs. [16,18], the authors suggested to use the standard streaming process for both species on two lattices, and exchange information between lattices with a second-order or higher order interpolation schemes at each time step, which is a rather tedious procedure. On the other hand, since the physical symmetry and lattice symmetry can be decoupled from each other in LBE [35], we can solve Eq. (4) using any standard numerical scheme. Here we use a second-order Lax-Wendroff scheme [8,36] to discretize Eq. (9) on the same lattice,

$$\begin{aligned} f_{\sigma i}(\boldsymbol{x}, t+\delta t) = {} & f_{\sigma i}^+(\boldsymbol{x},t) - \frac{A_\sigma}{2}[f_{\sigma i}^+(\boldsymbol{x}+\boldsymbol{c}_i \delta t, t) - f_{\sigma i}^+(\boldsymbol{x}-\boldsymbol{c}_i \delta t, t)] \\ & + \frac{A_\sigma^2}{2}[f_{\sigma i}^+(\boldsymbol{x}+\boldsymbol{c}_i \delta t, t) - 2 f_{\sigma i}^+(\boldsymbol{x},t) \\ & + f_{\sigma i}^+(\boldsymbol{x}-\boldsymbol{c}_i \delta t, t)], \end{aligned} \tag{15}$$

where the parameter A_σ is chosen to be $A_\sigma = c_\sigma / c$ with $c = \sqrt{3 k_B T / m} = \delta x / \delta t$, where m is the reference molecular weight, δx is the streaming step and δt is the time step. It is clear that the parameter A_σ depends on the molecular mass of species σ. Actually, A_σ is related to the mobility of the molecule. For heavy molecules, A_σ is small, but for light molecules, A_σ is large. The time step δt should be chosen according to some stability requirements as shown in Ref. [8],

$$\delta t \le \min\{2.0/\tilde{s}_{\sigma i}, \delta x / \sqrt{3 R_\sigma T}, \delta x / \sqrt{3 R_{\sigma'} T}\}. \tag{16}$$

Considering the discrete lattice effects in LBE, the forcing term $\tilde{F}_\sigma$ in Eq. (12) should be redefined as [29]

$$\tilde{F}_\sigma = \left(\boldsymbol{I} - \frac{\bar{\boldsymbol{S}}_\sigma}{2}\right) \tilde{F}_\sigma, \tag{17}$$

where $\bar{\boldsymbol{S}}_\sigma = diag\{s_{\sigma 1}, s_{\sigma 2}, \cdots, s_{\sigma 9}\}$ with $s_{\sigma i} = \tilde{s}_{\sigma i} \delta t$ being the nondimensional relaxation rate for species σ, and the flow variables for the mixtures are defined as

$$\rho_\sigma = \sum_i f_{\sigma i}, \quad \rho = \sum_\sigma \rho_\sigma, \quad \rho \boldsymbol{u} = \sum_{\sigma i} c_{\sigma i} f_{\sigma i} + \frac{\delta t}{2} \sum_\sigma \rho_\sigma \boldsymbol{a}_\sigma, \tag{18}$$

III. CHAPMAN-ENSKOG EXPANSION ANALYSIS

A. Hydrodynamic equation

We now analyze the hydrodynamic behavior of the MRT-LBE presented above using the Chapman-Enskog expansion procedure [37]. To this end, we first rewrite Eq. (15) as

$$f_{\sigma i}(\boldsymbol{x},t+\delta t)=f^{+}_{\sigma i}(\boldsymbol{x},t)-\delta t(c_{\sigma i}\cdot\nabla)f^{+}_{\sigma i}(\boldsymbol{x},t)+\frac{\delta t^2}{2}(c_{\sigma i}\cdot\nabla)^2 f^{+}_{\sigma i}(\boldsymbol{x},t)+O(\delta t^3), \quad (19)$$

and rewrite Eq. (12) in the velocity space as

$$f^{+}_{\sigma i}=f_{\sigma i}-\delta t S_{\sigma ij}(f_{\sigma j}-f^{(eq)}_{\sigma j})+\delta t F_{\sigma i}, \quad (20)$$

With Eqs. (19) and (20), we can obtain the following equation up to $O(\delta t^2)$:

$$D_{\sigma i}f_{\sigma i}+\frac{\delta t}{2}D^2_{\sigma i}f_{\sigma i}=-S_{\sigma ij}(f_{\sigma j}-f^{(eq)}_{\sigma j})+F_{\sigma i}, \quad (21)$$

where $D_{\sigma i}=\partial_t+c_{\sigma i}\cdot\nabla$. Then we introduce the following expansions:

$$f_{\sigma i}=f^{(0)}_{\sigma i}+\epsilon f^{(1)}_{\sigma i}+\epsilon^2 f^{(2)}_{\sigma i}+\cdots, \quad (22)$$

$$\partial_t=\epsilon\partial_{t_1}+\epsilon^2\partial_{t_2},\quad \nabla=\epsilon\nabla_1,\quad F_\sigma=\epsilon F_{1\sigma}, \quad (23)$$

where ϵ is a small parameter. With these expansions, Eq. (21) can be rewritten in consecutive orders of ϵ as

$$f^{(0)}_{\sigma i}=f^{(eq)}_{\sigma i},\quad O(\epsilon^0), \quad (24)$$

$$D^{(1)}_{\sigma i}f^{(0)}_{\sigma i}=-S_{\sigma ij}f^{(1)}_{\sigma j}+F_{1\sigma i},\quad O(\epsilon^1), \quad (25)$$

$$\partial_{t_2}f^{(0)}_{\sigma i}+D^{(1)}_{\sigma i}\left[\left(I_{ij}-\frac{S_{\sigma ij}}{2}\right)f^{(1)}_{\sigma j}\right]=-S_{\sigma ij}f^{(2)}_{\sigma j}-\frac{\delta t}{2}D^{(1)}_{\sigma i}F^{(1)}_{\sigma i},\quad O(\epsilon^2), \quad (26)$$

where $D^{(1)}_{\sigma i}=\partial_{t_1}+c_{\sigma i}\cdot\nabla_1$.

Multiplying the transformation matrix $\boldsymbol{M}$ on both side of Eqs. (24)–(26), we can obtain the following moment equations:

$$\boldsymbol{m}^{(0)}_\sigma=\boldsymbol{m}^{(eq)}_\sigma,\quad O(\epsilon^0), \quad (27)$$

$$[\partial_{t_1}+\boldsymbol{M}(\boldsymbol{c}_\sigma\cdot\nabla_1)\boldsymbol{M}^{-1}]\boldsymbol{m}^{(0)}_\sigma=-\tilde{\boldsymbol{S}}_\sigma\boldsymbol{m}^{(1)}_\sigma+\left(\boldsymbol{I}-\frac{\overline{\boldsymbol{S}}_\sigma}{2}\right)\tilde{F}_{1\sigma},\quad O(\epsilon), \quad (28)$$

$$\partial_{t_2}\boldsymbol{m}^{(0)}_\sigma+[\partial_{t_1}+\boldsymbol{M}(\boldsymbol{c}_\sigma\boldsymbol{I}\cdot\nabla_1)\boldsymbol{M}^{-1}]\left(\boldsymbol{I}-\frac{\tilde{\boldsymbol{S}}_\sigma}{2}\right)\boldsymbol{m}^{(1)}_\sigma=-\tilde{\boldsymbol{S}}_\sigma\boldsymbol{m}^{(2)}_\sigma-\frac{\delta t}{2}[\partial_{t_1}+\boldsymbol{M}(\boldsymbol{c}_\sigma\boldsymbol{I}\cdot\nabla_1)\boldsymbol{M}^{-1}]\left(\boldsymbol{I}-\frac{\overline{\boldsymbol{S}}_\sigma}{2}\right)\boldsymbol{F}_\sigma,\quad O(\epsilon^2). \quad (29)$$

With the results of Eqs. (27)–(29), the following conservation equations for component σ on the first and second orders can be recovered as

Continuity equations,

$$\partial_{t_1}\rho_\sigma+\partial_{1x}(\rho_\sigma u_x)+\partial_{1y}(\rho_\sigma u_y)=0, \quad (30)$$

$$\partial_{t_2}\rho_\sigma+\partial_{1x}\left[\delta t\left(1-\frac{s_{\sigma 4}}{2}\right)J^{(1)}_{\sigma x}\right]+\partial_{1y}\left[\delta t\left(1-\frac{s_{\sigma 6}}{2}\right)J^{(1)}_{\sigma y}\right]=0, \quad (31)$$

Momentum equations,

$$\partial_{t_1}(\rho_\sigma u_x)+\partial_{1x}[p_\sigma+\rho_\sigma u_x^2]+\partial_{1y}(\rho_\sigma u_x u_y)=-\tilde{s}_{\sigma 4}J^{(1)}_{\sigma x}+\rho_\sigma a_{\sigma x}, \quad (32)$$

$$\partial_{t_1}(\rho_\sigma u_y)+\partial_{1x}(\rho_\sigma u_x u_y)+\partial_{1y}[p_\sigma+\rho_\sigma u_y^2]=-\tilde{s}_{\sigma 6}J^{(1)}_{\sigma y}+\rho_\sigma a_{\sigma y}, \quad (33)$$

$$\begin{aligned}\partial_{t_2}(\rho_\sigma u_x)&+\partial_{1x}\left[\frac{1}{6}\left(1-\frac{s_{\sigma 2}}{2}\right)e^{(1)}_\sigma+\frac{1}{2}\left(1-\frac{s_{\sigma 8}}{2}\right)p^{(1)}_{\sigma xx}\right]+\partial_{1y}\left[\left(1-\frac{s_{\sigma 9}}{2}\right)p^{(1)}_{\sigma xy}\right]=-s_{\sigma 4}j^{(2)}_{\sigma x}-\left(1-\frac{s_{\sigma 4}}{2}\right)\partial_{t_1}J^{(1)}_{\sigma x}\\&-\partial_x\left[\frac{\delta t}{2}\left(1-\frac{s_{\sigma 2}}{2}\right)\rho_\sigma(a_{\sigma x}u_x+a_{\sigma y}u_y)+\frac{\delta t}{2}\left(1-\frac{s_{\sigma 8}}{2}\right)\rho_\sigma(a_{\sigma x}u_x-a_{\sigma y}u_y)\right]\\&-\partial_y\left[\frac{\delta t}{2}\left(1-\frac{s_{\sigma 9}}{2}\right)\rho_\sigma(a_{\sigma x}u_y-a_{\sigma y}u_x)\right],\end{aligned} \quad (34)$$

$$\begin{aligned}\partial_{t_2}(\rho_\sigma u_y)&+\partial_{1x}\left[\left(1-\frac{s_{\sigma 9}}{2}\right)p^{(1)}_{\sigma xy}\right]+\partial_{1y}\left[\frac{1}{6}\left(1-\frac{s_{\sigma 2}}{2}\right)e^{(1)}_\sigma-\frac{1}{2}\left(1-\frac{s_{\sigma 8}}{2}\right)\frac{p^{(1)}_{\sigma xx}}{2}\right]=-s_{\sigma 6}j^{(2)}_{\sigma y}-\left(1-\frac{s_{\sigma 6}}{2}\right)\partial_{t_1}J^{(1)}_{\sigma y}\\&-\partial_x\left[\frac{\delta t}{2}\left(1-\frac{s_{\sigma 9}}{2}\right)\rho_\sigma(a_{\sigma x}u_y-a_{\sigma y}u_x)\right]+\partial_y\left[\frac{\delta t}{2}\left(1-\frac{s_{\sigma 2}}{2}\right)\rho_\sigma(a_{\sigma x}u_x+a_{\sigma y}u_y)-\frac{\delta t}{2}\left(1-\frac{s_{\sigma 8}}{2}\right)\rho_\sigma(a_{\sigma x}u_x-a_{\sigma y}u_y)\right],\end{aligned} \quad (35)$$

where $p_\sigma=\rho_\sigma R_\sigma T$ is the partial pressure; $e^{(1)}_\sigma$, $p^{(1)}_{\sigma xx}$, $p^{(1)}_{\sigma xy}$, $\boldsymbol{j}^{(1)}_\sigma$, and $\boldsymbol{j}^{(2)}_\sigma$ are the corresponding moments expansions, i.e., $e_\sigma=\Sigma_k\epsilon^k e^{(k)}_\sigma=\Sigma_k\epsilon^k c^2_\sigma m^{(k)}_{\sigma 1}$, $p_{\sigma xx}=\Sigma_k\epsilon^k p^{(k)}_{\sigma xx}=\Sigma_{i,k}\epsilon^k c^2_{\sigma x}f^{(k)}_{\sigma i}$, $p_{\sigma xy}=\Sigma_k\epsilon^k p^{(k)}_{\sigma xy}=\Sigma_{i,k}\epsilon^k c_{\sigma x}c_{\sigma y}f^{(k)}_{\sigma i}$, $\boldsymbol{J}^{(0)}_\sigma=\boldsymbol{j}^{(0)}_\sigma=0$, $\boldsymbol{J}^{(1)}_\sigma=\boldsymbol{j}^{(1)}_\sigma=\Sigma_i\boldsymbol{c}_{\sigma i}f^{(1)}_{\sigma i}+\rho_\sigma\boldsymbol{a}_\sigma\delta t/2$, $\boldsymbol{J}^{(k)}_\sigma=\boldsymbol{j}^{(k)}_\sigma=\Sigma_i\boldsymbol{c}_{\sigma i}f^{(k)}_{\sigma i}$, $(k>1)$, where e_σ is related to the total energy, $p_{\sigma\alpha\beta}$ is the partial stress, $\boldsymbol{j}_\sigma$ the mass diffusive flux, and $\boldsymbol{J}_\sigma$ the effective mass diffusive flux.

To close the hydrodynamic equations at the second order of ϵ, the terms of $e^{(1)}_\sigma$, $p^{(1)}_{\sigma xx}$, $p^{(1)}_{\sigma xy}$ in Eqs. (34) and (35) should be determined. To this end, we now evaluate the terms of $\partial_{t_1}(\rho_\sigma u_x^2)$, $\partial_{t_1}(\rho_\sigma u_y^2)$, and $\partial_{t_1}(\rho_\sigma u_x u_y)$ using Eqs. (30)–(33), and obtain that

$$\partial_{t_1}(\rho_\sigma u_x^2) = -2u_x[\partial_{1x}p_\sigma + \tilde{s}_{\sigma 4}J_{\sigma x}^{(1)} - \rho_\sigma a_{\sigma x}] + O(u^3), \quad (36)$$

$$\partial_{t_1}(\rho_\sigma u_y^2) = -2u_y[\partial_{1y}p_\sigma + \tilde{s}_{\sigma 6}J_{\sigma y}^{(1)} - \rho_\sigma a_{\sigma y}] + O(u^3), \quad (37)$$

$$\partial_{t_1}(\rho_\sigma u_x u_y) = -u_x[\partial_{1y}p_\sigma + \tilde{s}_{\sigma 4}J_{\sigma y}^{(1)} - \rho_\sigma a_{\sigma y}] - u_y[\partial_{1x}p_\sigma + \tilde{s}_{\sigma 4}J_{\sigma x}^{(1)} - \rho_\sigma a_{\sigma x}] + O(u^3). \quad (38)$$

Then $\tilde{s}_{\sigma 2}e_\sigma^{(1)}$ can be expressed as

$$\tilde{s}_{\sigma 2}e_\sigma^{(1)} = -3\tilde{s}_{\sigma 2}\rho_\sigma(a_{\sigma x}u_x + a_{\sigma y}u_y) - 2\rho_\sigma c_\sigma^2(\partial_{1x}u_x + \partial_{1y}u_y) + 6(\tilde{s}_{\sigma 4}u_x J_{\sigma x}^{(1)} + \tilde{s}_{\sigma 6}u_y J_{\sigma y}^{(1)}). \quad (39)$$

Similarly, we have

$$\tilde{s}_{\sigma 8}p_{\sigma xx}^{(1)} = -\tilde{s}_{\sigma 8}\rho_\sigma(a_{\sigma x}u_x - a_{\sigma y}u_y) - \frac{2}{3}\rho_\sigma c_\sigma^2(\partial_{1x}u_x - \partial_{1y}u_y) + 2(\tilde{s}_{\sigma 4}u_x J_{\sigma x}^{(1)} - \tilde{s}_{\sigma 6}u_y J_{\sigma y}^{(1)}), \quad (40)$$

$$\tilde{s}_{\sigma 9}p_{\sigma xy}^{(1)} = -\frac{\tilde{s}_{\sigma 9}}{2}\rho_\sigma(a_{\sigma x}u_y + a_{\sigma y}u_x) - \frac{1}{3}\rho_\sigma c_\sigma^2(\partial_{1x}u_y + \partial_{1y}u_x) + \tilde{s}_{\sigma 6}u_x J_{\sigma y}^{(1)} + \tilde{s}_{\sigma 4}u_y J_{\sigma x}^{(1)}. \quad (41)$$

With Eqs. (39)–(41), we can obtain the hydrodynamic equations for the mixtures at t_1 and t_2 scales,

Continuity equations,

$$\partial_{t_1}\rho + \nabla_1 \cdot (\rho \boldsymbol{u}) = 0, \quad (42)$$

$$\partial_{t_2}\rho + \partial_{1x}\sum_\sigma\left[\left(1 - \frac{s_{\sigma 4}}{2}\right)J_{\sigma x}^{(1)}\right] + \partial_{1y}\sum_\sigma\left[\left(1 - \frac{s_{\sigma 6}}{2}\right)J_{\sigma y}^{(1)}\right] = 0, \quad (43)$$

Momentum equations,

$$\partial_{t_1}(\rho \boldsymbol{u}) + \nabla_1 \cdot (p\boldsymbol{I} + \rho \boldsymbol{u}\boldsymbol{u}) = \sum_\sigma \rho_\sigma \boldsymbol{a}_\sigma, \quad (44)$$

$$\partial_{t_2}(\rho u_x) - \partial_{1x}\left[\rho\xi(\partial_{1x}u_x + \partial_{1y}u_y) + \rho\nu(\partial_{1x}u_x - \partial_{1y}u_y) + \sum_\sigma\left(\frac{1}{s_{\sigma 2}} - \frac{1}{2}\right)(s_{\sigma 4}u_x J_{\sigma x}^{(1)} + s_{\sigma 6}u_y J_{\sigma y}^{(1)}) + \sum_\sigma\left(\frac{1}{s_{\sigma 8}} - \frac{1}{2}\right) \times (s_{\sigma 4}u_x J_{\sigma x}^{(1)} - s_{\sigma 6}u_y J_{\sigma y}^{(1)})\right] - \partial_{1y}\left[\rho\nu(\partial_{1x}u_y + \partial_{1y}u_x) + \sum_\sigma\left(\frac{1}{s_{\sigma 9}} - \frac{1}{2}\right)(s_{\sigma 4}u_y J_{\sigma x}^{(1)} + s_{\sigma 6}u_x J_{\sigma y}^{(1)})\right] = 0, \quad (45)$$

$$\partial_{t_2}(\rho u_y) - \partial_{1x}\left[\rho\nu(\partial_{1x}u_y + \partial_{1y}u_x) + \sum_\sigma\left(\frac{1}{s_{\sigma 9}} - \frac{1}{2}\right)(s_{\sigma 4}u_y J_{\sigma x}^{(1)} + s_{\sigma 6}u_x J_{\sigma y}^{(1)})\right] - \partial_{1y}\left[\rho\xi(\partial_{1x}u_x + \partial_{1y}u_y) - \rho\nu(\partial_{1x}u_x - \partial_{1y}u_y) + \sum_\sigma\left(\frac{1}{s_{\sigma 2}} - \frac{1}{2}\right)(s_{\sigma 4}u_x J_{\sigma x}^{(1)} + s_{\sigma 6}u_y J_{\sigma y}^{(1)}) - \sum_\sigma\left(\frac{1}{s_{\sigma 8}} - \frac{1}{2}\right) \times (s_{\sigma 4}u_x J_{\sigma x}^{(1)} - s_{\sigma 6}u_y J_{\sigma y}^{(1)})\right] = 0, \quad (46)$$

where the shear viscosity and bulk viscosity of the mixture are defined by

$$\rho\nu = \sum_\sigma \rho_\sigma \nu_\sigma = \sum_\sigma p_\sigma\left(\frac{1}{s_{\sigma 8}} - \frac{1}{2}\right)\delta t = \sum_\sigma p_\sigma\left(\frac{1}{s_{\sigma 9}} - \frac{1}{2}\right)\delta t, \quad (47)$$

$$\rho\xi = \sum_\sigma \rho_\sigma \xi_\sigma = \sum_\sigma p_\sigma\left(\frac{1}{s_{\sigma 2}} - \frac{1}{2}\right)\delta t. \quad (48)$$

In Eq. (43), the two terms associated with the diffusive flux $\boldsymbol{J}_\sigma^{(1)}$ should vanish in order to obtain the correct continuity equation for the mixture. This can be achieved by setting $s_{\sigma 4}=s_{\sigma 6}=s_4$. In the momentum equations [Eqs. (45) and (46)], the terms associated with $\boldsymbol{J}_\sigma^{(1)}$ can also be neglected because the diffusion velocities can be assumed to be much smaller than the averaged velocity, as argued in Ref. [14]. As such, we can obtain the following mass and momentum conservation equations for the mixture by combining Eqs. (42)–(46) at t_1 and t_2 scales,

$$\partial_t \rho + \nabla \cdot (\rho \boldsymbol{u}) = 0, \quad (49)$$

$$\partial_t(\rho \boldsymbol{u}) + \nabla \cdot (\rho \boldsymbol{u}\boldsymbol{u} + p\boldsymbol{I}) = \nabla \cdot \tau + \sum_\sigma \rho_\sigma \boldsymbol{a}_\sigma, \quad (50)$$

where the pressure and stress of the mixture are given by

$$p = \sum_\sigma p_\sigma, \quad \tau = \rho\nu[\nabla \boldsymbol{u} + (\nabla \boldsymbol{u})^T] - \rho\xi\nabla \cdot \boldsymbol{u}\boldsymbol{I}, \quad (51)$$

where ν and ξ are defined by Eqs. (47) and (48), respectively. Therefore, the proposed FD-LBE can be applied to mixtures with different species viscosities by adjusting $s_{\sigma 8}$.

B. Diffusion equation

In order to obtain the diffusion equation, we first evaluate the effective mass diffusive flux $\boldsymbol{J}_\sigma$. Using Eq. (30), we can rewrite Eqs. (32), (33), and (44) as

$$\rho_\sigma(\partial_{t_1}\boldsymbol{u} + \boldsymbol{u} \cdot \nabla_1 \boldsymbol{u}) = -\nabla_1 p_\sigma - \tilde{s}_4 \boldsymbol{J}_\sigma^{(1)} + \rho_\sigma \boldsymbol{a}_\sigma, \quad (52)$$

$$\rho(\partial_{t_1}\boldsymbol{u} + \boldsymbol{u} \cdot \nabla_1 \boldsymbol{u}) = -\nabla_1 p + \sum_\sigma \rho_\sigma \boldsymbol{a}_\sigma. \quad (53)$$

Then $\tilde{s}_4 \boldsymbol{J}_\sigma^{(1)}$ can be expressed as

$$\tilde{s}_4 \boldsymbol{J}_\sigma^{(1)} = \frac{\rho_\sigma \rho_{\sigma'}}{\rho}(\boldsymbol{a}_\sigma - \boldsymbol{a}_{\sigma'}) - \nabla p_\sigma + \frac{\rho_\sigma \nabla p}{\rho}. \quad (54)$$

The terms on the right hand of Eq. (54) imply three different driving mechanisms: the difference in the external forces, the concentration gradients, and the pressure gradients acting on different species. These driving mechanisms are usually called forced diffusion, ordinary diffusion, and pressure diffusion, respectively. If there is no external force ($\boldsymbol{a}_\sigma = \boldsymbol{a}_{\sigma'} = 0$) and the system is at mechanical equilibrium (p is a con-

stant), Eq. (54) can be rewritten in the form of Fick's law as

$$\left(1-\frac{s_4}{2}\right)\boldsymbol{J}_\sigma^{(1)} = -\nabla p_\sigma\left(\frac{1}{s_4}-\frac{1}{2}\right)\delta t = -\rho D_{\sigma\sigma'}\nabla X_\sigma, \quad (55)$$

where $X_\sigma=\rho_\sigma/\rho$ is the mass fraction of species σ, and the mutual diffusion coefficient $D_{\sigma\sigma'}$ is given by

$$D_{\sigma\sigma'} = \frac{\rho p}{n^2 m_\sigma m_{\sigma'}}\left(\frac{1}{s_4}-\frac{1}{2}\right)\delta t. \quad (56)$$

As indicated in Eq. (56), we can obtain the self-diffusivity for species σ as

$$D_{\sigma\sigma} = R_\sigma T\left(\frac{1}{s_4}-\frac{1}{2}\right)\delta t. \quad (57)$$

From Eqs. (47) and (56), it is clear that the Schmidt number of the mixture, $\mathrm{Sc}=\nu/D_{\sigma\sigma'}$, can be adjusted by tuning s_4, $s_{\sigma 8}$, and $s_{\sigma' 8}$.

On the other hand, from Eqs. (30) and (31), the continuity equation for species σ can be rewritten as

$$\rho(\partial_t X_\sigma + \boldsymbol{u}\cdot\nabla X_\sigma) = -\nabla\cdot\left[\left(1-\frac{s_4}{2}\right)\boldsymbol{J}_\sigma\right], \quad (58)$$

and then combining with Eq. (55), we can get the following diffusion equation:

$$\rho(\partial_t X_\sigma + \boldsymbol{u}\cdot\nabla X_\sigma) = \nabla\cdot(\rho D_{\sigma\sigma'}\nabla X_\sigma). \quad (59)$$

IV. BOUNDARY CONDITIONS

Boundary conditions for LBE method have been studied extensively [38]. In this work, we will extend the nonequilibrium-extrapolation method for single-component flows [39] to the proposed MRT-LBE model.

The basic idea of the nonequilibrium extrapolation can be interpreted as follows. The distribution function for species σ at a boundary node x_B can be decomposed into an equilibrium part and a nonequilibrium part, that is

$$f_{\sigma i}(x_B,t) = f_{\sigma i}^{(eq)}(x_B,t) + f_{\sigma i}^{(neq)}(x_B,t).$$

The boundary conditions are then enforced through the equilibrium part, while the nonequilibrium part is determined by using certain extrapolation schemes. For instance, for a boundary where $\boldsymbol{u}(x_B,t)$ is known but $\rho_\sigma(x_B,t)$ is unknown, we use a temporary density $\bar{\rho}_\sigma(x_B,t)$ instead of $\rho_\sigma(x_B,t)$ in the evaluation of the equilibrium distribution function, i.e.,

$$\bar{\rho}_\sigma(x_B,t) = \rho_\sigma(x_f,t),$$

where x_f is the nearest node of x_B. As such, the equilibrium distribution function for species σ at x_B can be approximated as

$$f_{\sigma i}^{(eq)}(x_B,t) = f_{\sigma i}^{(eq)}[\bar{\rho}_\sigma(x_B,t),\boldsymbol{u}(x_B,t)].$$

For the nonequilibrium part, we can approximate it by the nonequilibrium part of the neighboring node x_f.

$$f_{\sigma i}^{(neq)}(x_B,t) = f_{\sigma i}(x_f,t) - f_{\sigma i}^{(eq)}(x_f,t).$$

Finally, the distribution function for species σ at the boundary node x_B can be approximated as

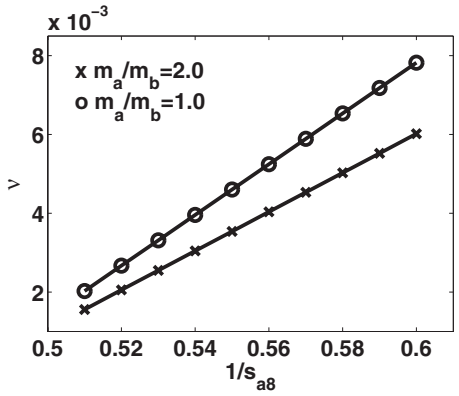

FIG. 1. Shear viscosity as a function of the relaxation rate s_{a8} with $s_{b8}^{-1}=0.55$, $X_a=0.7$ and $X_b=0.3$. Symbols are the FD-MRT results, and solid lines are the theoretical predictions given by Eq. (47).

$$f_{\sigma i}(x_B,t) = f_{\sigma i}^{(eq)}(x_B,t) + [f_{\sigma i}(x_f,t) - f_{\sigma i}^{(eq)}(x_f,t)] \quad (60)$$

V. NUMERICAL TESTS

In this section, some numerical tests will be presented to validate the proposed LBE model. In simulations, the relaxation rates are set as follows. For the conserved moment (species densities), we take $s_{\sigma 1}=0$, while $s_{\sigma 8}=s_{\sigma 9}$ and $s_{\sigma 4}=s_{\sigma 6}=s_4$ are determined from the prescribed shear viscosities and diffusivity, respectively, and the remaining relaxation rates are all set to be unity.

We first test the shear viscosity ν of the model by measuring the decay rate of a sinusoidal perturbation in velocity with small amplitude. In our simulations, a 128×128 lattice is used, and periodic boundary conditions are applied to both directions. The measured shear viscosity in two cases, namely $m_a/m_b=1$ and $m_a/m_b=2$ with $m_b=1.0$, $A_a=1.0$ and $c=10$, are shown in Figs. 1 and 2, respectively. It is clearly seen that ν is a function of s_{a8} and s_{b8}, which agrees well with the theoretical results given by Eq. (47). It should be noted that the shear viscosity in Figs. 1 and 2 are quite dif-

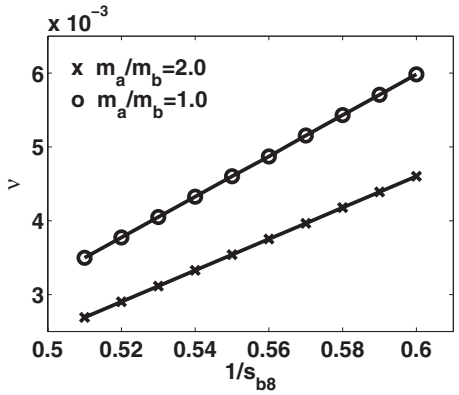

FIG. 2. Shear viscosity as a function of the relaxation rate s_{b8} with $s_{a8}^{-1}=0.55$, $X_a=0.7$ and $X_b=0.3$. Symbols are the FD-MRT results, and the solid lines are the theoretical predictions given by Eq. (47).

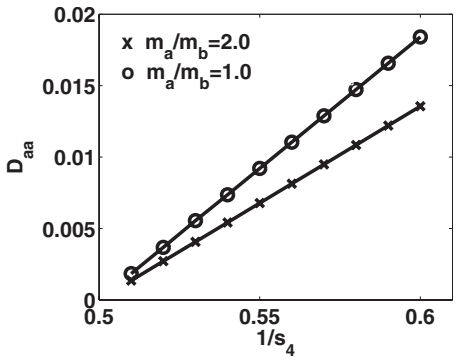

FIG. 3. Self-diffusivity as a function of the relaxation rate. Symbols are the FD-MRT results, and solid lines are theoretical predictions given by Eq. (57).

ferent for the same mass ratios. The reason for this phenomenon is that each species has different mass fraction (X_a =0.7 and X_b=0.3) in our simulations, and as shown by Eq. (45), the viscosity ν also depends on the species concentration. Therefore, if $X_a \neq X_b$, $\nu(s_{a8})$ will be different to $\nu(s_{b8})$ in general.

We now test the self-diffusion coefficient D_{aa} of the proposed LBE model. The test case is the same as that used in Refs. [13,21]. In simulations periodic boundary conditions are applied to both directions with a perturbed initial density distribution along the x direction,

$$\rho_a(x,0) = \bar{\rho}_a[1 + \delta_a \sin(kx)], \tag{61}$$

$$\rho_b(x,0) = \bar{\rho}_b[1 - \delta_b \sin(kx)], \tag{62}$$

where $\bar{\rho}_a$=0.64, $\bar{\rho}_b$=1.15, $\delta_a=\delta_b$=0.001, and $k=2\pi/L$ is the wave number of the perturbation. In this case, the density ρ_a and ρ_b have the following sine-wave density profiles:

$$\rho_a(x,t) = \bar{\rho}_a[1 + \delta_a \sin(kx)]e^{-D_{aa}k_x^2 t}, \tag{63}$$

$$\rho_b(x,t) = \bar{\rho}_b[1 - \delta_b \sin(kx)]e^{-D_{bb}k_x^2 t}. \tag{64}$$

The measured self-diffusivity D_{aa} and the theoretical predictions are shown in Fig. 3 for two cases (m_a/m_b=1 and m_a/m_b=2). It is seen again that the numerical results agree well with the theoretical ones given by Eq. (57). In addition, we also found that the present LBE exhibits excellent numerical stability. Actually, the computation is still stable even as $m_a/m_b \geq 10^6$.

To further evaluate the proposed model, two gases with large different molecular weights diffusing into each other are also investigated. Initially, we set T=273 K and p_0 =1 bar, and the density of each species is assumed to have a hyperbolic tangent profile [16,21],

$$\rho_a(y,t=0) = \frac{1}{2}\left[(\rho_{ah} + \rho_{al}) + (\rho_{ah} - \rho_{al})\tanh\left(\frac{y - H/2}{\delta_{th}}\right)\right], \tag{65}$$

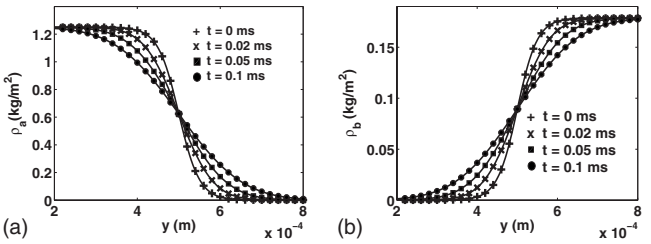

FIG. 4. Density profiles of the species at different times. Symbols are the FD-MRT results, and solid lines are the predictions of Ref. [16] at t=0, 0.02, 0.05, and 0.1 ms, respectively.

$$\rho_b(y,t=0) = \frac{1}{2}\left[(\rho_{bh} + \rho_{bl}) + (\rho_{bl} - \rho_{bh})\tanh\left(\frac{y - H/2}{\delta_{th}}\right)\right], \tag{66}$$

where $0 \leq y \leq H$, H is the width of the computational domain and δ_{th} is the thickness of the diffusion profile. In this case, we study the diffusion between nitrogen and helium gases, the parameters of these two gases are the same as Ref. [16], i.e., the maximum and minimum density values of each species are ρ_{ah}=1.250 kg/m^2, ρ_{bh}=0.179 kg/m^2, ρ_{al} =0.0007 kg/m^2 and ρ_{bl}=0.0001 kg/m^2 with δ_{th}=0.05 mm, and the binary diffusivity of helium and nitrogen at this temperature is D_{ab}=0.632 cm^2/s. In our simulations, a lattice of size $N_x \times N_y = 10 \times 500$ is employed, and the corresponding lattice spacing and time step are δx=2 μm and δt=3 ns, respectively. Periodic boundary condition is applied to the x direction and the nonequilibrium-extrapolation method is applied to the horizontal boundaries.

In Fig. 4, the density distributions of both species predicted by the proposed MRT-LBE model are compared with the results of the Ref. [16] at t=0, 0.02, 0.05, and 0.1 ms, respectively. It is observed from Fig. 4 that both numerical solutions are in excellent agreement, indicating that the diffusion phenomena can be correctly described by the present model. Nevertheless, we found that the mass ratio and the thickness δ_{th} have influences on the numerical stability. For instance, when the thickness is set to be δ_{th}=0.05 mm, the computation is stable even as $m_a/m_b \geq 10^4$. However, as $\delta_{th}=10^{-30}$ mm, the computation becomes unstable as $m_a/m_b > 95$.

We also test the proposed LBE model using a mixture with a sharp interface. The mass ratio is set to be as high as m_b/m_a=500. The initial conditions are the same as the Ref. [18] but the diffusivity is D_{ab}=0.05. Initially the molar concentration $Y_\sigma = n_\sigma/n$ is given by

$$Y_a = 90\%, \quad Y_b = 10\% \quad \text{if } y < 0,$$

$$Y_a = 10\%, \quad Y_b = 90\% \quad \text{if } y \geq 0. \tag{67}$$

The boundary conditions and grid resolution are the same as those used in the above smooth profiles test. For this case, the analytical transient solution is [18]

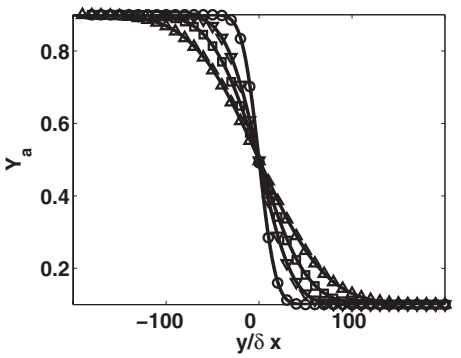

FIG. 5. Concentration profiles of the species at different times. Symbols are the LBE results, and solid lines are theoretical predictions given by Eq. (68) at time step 10 000 (○);40 000 (▽), 80 000 (□), 160 000 (△).

$$Y_\sigma = \frac{1}{2} + \frac{\delta Y_\sigma}{2}\mathrm{erf}\left(\frac{y}{2\sqrt{D_{\sigma\sigma'}t}}\right), \tag{68}$$

where δY_σ is the initial fraction difference, and erf is the error function. The comparison between the numerical results and the analytical solutions are presented in Fig. 5, and good agreement is observed. However, it is found that when the initial concentration difference of the two species is above a critical value, say $Y_a=92\%$ and $Y_b=8\%$, numerical instability will occur.

Finally, we investigate the achievable Schmidt number of the proposed LBE. A mixture flow of two species with identical molecular weights between two parallel plates is considered. Initially, the species concentration is given by Eq. (60). The flow is driven by external forces $\boldsymbol{a}_a=\boldsymbol{a}_b=(a_x,a_y)=(0.0001,0)$. Simulations are carried out on a 4×200 mesh. Periodic boundary condition is applied to the x direction and nonslip boundary condition is applied to the two horizontal walls.

It can be shown that the barycentric velocity of this flow is

$$u = \frac{a_x H}{2\nu} y\left(1 - \frac{y}{H}\right). \tag{69}$$

With this analytical solution, we can measure the kinematic viscosity following the idea of Refs. [20,40]. The mutual diffusivity can be obtained by fitting the numerical data using a function of the form Eq. (68).

In our tests the following values of ν and D_{ab} are used:

$$\nu = \{0.1,1,3,5,10,15,20,25\}, \tag{70}$$

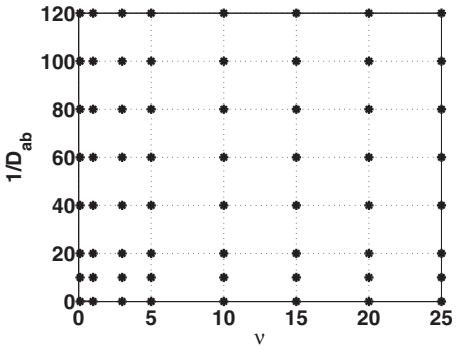

FIG. 6. Transport coefficients of the measured ν and D_{ab}. Asterisk means the numerical error in Schmidt number is lower than 5%.

$$D_{ab}^{-1} = \{0.001,10,20,40,60,80,100,120\}, \tag{71}$$

The measured Schmidt numbers are shown in Fig. 6, where the corresponding transport coefficients is marked when the numerical error between measured coefficients and the given values [Eqs. (70) and (71)] is lower than 5%. It is found that the measured Schmidt number is reliable in a large range. We also investigate the case of $m_a/m_b=20$ with $\nu=1$, and found that the computation is stable as $\mathrm{Sc}\geq0.012$.

VI. SUMMARY

In this paper, we have proposed a FD-LBE model for binary mixtures. The model has two distinctive features in comparison with previous LBE models. First, the streaming process is realized based on a Lax-Wendroff scheme, and thus particles with different molecular weights can stream on the same lattice. Second, owing to the use of the MRT collision operator, the model can be applied to the mixtures with different individual viscosities and adjustable Schmidt number.

Some numerical simulations have been carried out to validate the proposed model. It is found that the numerical results are in excellent agreement with the analytical solutions and/or other numerical results. It is also demonstrated that the present LBE model has a good numerical stability and is insensitive to the mass ratio.

ACKNOWLEDGMENTS

The authors are grateful to Professor P. Asinari for many helpful discussions. This work is supported by the National Natural Science Foundation of China (Grant No. 10972087) and the National Basic Research Programme of China (under Grant No. 2006CB705800). Z.L. Guo was also supported by the open grant from the State Key Laboratory of EOR.

[1] R. Benzi, S. Succi, and M. Vergassola, Phys. Rep. **222**, 145 (1992).

[2] S. Succi, *The Lattice Boltzmann Equation for Fluid Dynamics and Beyond* (Oxford Univiversity Press, Oxford, 2001).

[3] S. Chen and G. Doolen, Annu. Rev. Fluid Mech. **30**, 329 (1998).

[4] A. K. Gunstensen, D. H. Rothman, S. Zaleski, and G. Zanetti, Phys. Rev. A **43**, 4320 (1991).

[5] X. Shan and G. Doolen, J. Stat. Phys. **81**, 379 (1995).
[6] X. Shan and G. Doolen, Phys. Rev. E **54**, 3614 (1996).
[7] M. R. Swift, W. R. Osborn, and J. M. Yeomans, Phys. Rev. Lett. **75**, 830 (1995); M. R. Swift, E. Orlandini, W. R. Osborn, and J. M. Yeomans, Phys. Rev. E **54**, 5041 (1996).
[8] Z. L. Guo and T. S. Zhao, Phys. Rev. E **68**, 035302(R) (2003); **71**, 026701 (2005).
[9] A. G. Xu, G. Gonnella, and A. Lamura, Phys. Rev. E **67**, 056105 (2003).
[10] V. Sofonea, A. Lamura, G. Gonnella, and A. Cristea, Phys. Rev. E **70**, 046702 (2004).
[11] V. Sofonea and R. F. Sekerka, Int. J. Mod. Phys. C **16**, 1075 (2005).
[12] V. Sofonea, Int. J. Mod. Phys. C **19**, 677 (2008).
[13] P. Asinari and L.-S. Luo, J. Comput. Phys. **227**, 3878 (2008).
[14] L.-S. Luo and S. S. Girimaji, Phys. Rev. E **66**, 035301(R) (2002); **67**, 036302 (2003).
[15] A. G. Xu, Phys. Rev. E **71**, 066706 (2005).
[16] M. E. McCracken and J. Abraham, Phys. Rev. E **71**, 046704 (2005).
[17] M. E. McCracken and J. Abraham, Int. J. Mod. Phys. C **16**, 533 (2005).
[18] S. Arcidiacono, J. Mantzaras, S. Ansumali, I. V. Karlin, C. Frouzakis, and K. B. Boulouchos, Phys. Rev. E **74**, 056707 (2006).
[19] S. Arcidiacono, I. V. Karlin, J. Mantzaras, and C. E. Frouzakis, Phys. Rev. E **76**, 046703 (2007).
[20] P. Asinari, Phys. Fluids **17**, 067102 (2005).
[21] P. Asinari, Phys. Rev. E **73**, 056705 (2006).
[22] V. Sofonea and R. F. Sekerka, Physica A **299**, 494 (2001).
[23] P. L. Bhatnagar, E. P. Gross, and M. Krook, Phys. Rev. **94**, 511 (1954).
[24] L. Sirovich, Phys. Fluids **5**, 908 (1962).
[25] P. Andries, K. Aoki, and B. Perthame, J. Stat. Phys. **106**, 993 (2002).
[26] B. B. Hamel, Phys. Fluids **8**, 418 (1965); **9**, 12 (1966).
[27] H. Grad, in *Rarefied Gas Dynamics*, edited by F. Devienne (Pergamon, London, 1960).
[28] T. F. Morse, Phys. Fluids **7**, 2012 (1964).
[29] Z. L. Guo, C. G. Zheng, and B. C. Shi, Phys. Rev. E **65**, 046308 (2002).
[30] Z. L. Guo, C. G. Zheng, B. C. Shi, and T. S. Zhao, Phys. Rev. E **75**, 036704 (2007).
[31] D. d'Humières, in *Rarefied Gas Dynamics: Theory and Simulations, Progress in Astronautics and Aeronautics*, edited by B. D. Shizgal and D. P. Weaver (AIAA, Washington, DC, 1992), Vol. 159, p. 450.
[32] P. Lallemand and L.-S. Luo, Phys. Rev. E **61**, 6546 (2000).
[33] D. d'Humières, M. Bouzidi, and P. Lallemand, Phys. Rev. E **63**, 066702 (2001).
[34] L. Zheng, B. C. Shi, and Z. L. Guo, Phys. Rev. E **78**, 026705 (2008).
[35] N. Cao, S. Chen, S. Jin, and D. Martinez, Phys. Rev. E **55**, R21 (1997).
[36] Z. L. Guo, C. G. Zheng, and T. S. Zhao, J. Sci. Comput. **16**, 569 (2001).
[37] S. Chapman and T. G. Cowling, *The Mathematical Theory of Non-uniform Gases*, 3rd ed. (Cambridge University Press, Cambridge, England, 1970).
[38] X. He, Q. Zou, and L.-S. Luo, J. Stat. Phys. **87**, 115 (1997).
[39] Z. L. Guo, C. G. Zheng, and B. C. Shi, Phys. Fluids **14**, 2007 (2002).
[40] P. Asinari, Phys. Rev. E **77**, 056706 (2008).